Scientific paper

Study of Thermal Decomposition of $(K_{0.5}Na_{0.5})NbO_3$ Thin-films Precursors with Different Amounts of Alkali-acetate Excess

Alja Kupec,[1,2,*] Oana Cătălina Mocioiu,[3,*] Jena Cilenšek,[1] Maria Zaharescu[3] and Barbara Malič[1,2]

[1] *Jožef Stefan Institute, Jamova cesta 39, 1000 Ljubljana, Slovenia*

[2] *Jožef Stefan International Postgraduate School, Jamova cesta 39, 1000 Ljubljana, Slovenia*

[3] *"Ilie Murgulescu" Institute of Physical Chemistry of Romanian Academy, 202 Splaiul Independentei, Bucharest 060021, Romania*

* *Corresponding author: E-mail: alja.kupec@ijs.si; oana.mocioiu@gmail.com*

Dedicated to the memory of Prof. Dr. Marija Kosec.

Abstract

Liquid precursors of $(K_{0.5}Na_{0.5})NbO_3$ thin-films were prepared from alkali acetates and niobium ethoxide in 2-methoxyethanol solvent either in a stoichiometric ratio or with 5 or 10 mole % of potassium or sodium acetate excess. Fourier-transform infrared (FTIR) spectroscopy of the dried precursors confirmed the presence of acetate and hydroxyl groups. Thermal decompositions of the as-dried precursors in air occurred gradually. Between room temperature and ~200 °C, the weight loss of a few per cent was due to the evaporation of residual solvents. The major mass loss was due to thermal oxidation of organic group with the major exothermic events at about 250 °C and 450 °C, almost 200 °C below the onset of the chemical decomposition of alkali acetates, indicating that a heterometallic complex was formed in solution, in agreement with FTIR analysis. Both the amount and to a lesser extent the choice of alkali-acetate excess influenced the thermal decomposition of the organic groups predominantly in the temperature interval between ~200 °C and ~400 °C.

Keywords: Lead-free, Alkaline Niobates, Thermal analysis, Fourier-transform infrared spectroscopy

1. Introduction

Lead-free piezoelectric ceramics have been the topic of intensive research since early 2000's due to the increased awareness of both health- and environment hazards related to fabrication, use and disposal of lead-based piezoelectrics.[1] In addition to studies of bulk piezoelectric and ferroelectric ceramics, the research of thin films has been promoted by miniaturization trends in electronics and microelectromechanical systems.[2,3]

Sodium potassium niobate with the alkali metal molar ratio equal to 1 $(K_{0.5}Na_{0.5})NbO_3$ (KNN) has been one of the intensively studied lead-free materials compositions, which could replace human- and environment-hazardous lead-ba-

sed perovskites.[4,5] Processing problems related to KNN films have been reported, and they are related to humidity sensitivity of reagents, ease of formation of non-perovskite phases upon heating, volatility of alkali oxides at the processing temperatures, and consequent loss of stoichiometry and degraded functional properties, to name only some.[6–11]

In Chemical Solution Deposition of thin films, the possible loss of alkalis upon heating could be compensated by the addition of excess of alkali compounds in the coating solution. In different studies, the latter varied from no excess (0) to 20 mole %, nevertheless, the films crystallized in perovskite phase[9–11] In our previous work we prepared KNN thin films from acetate-alkoxide based solutions containing 0, 5 or 10 mole % of sodium or potassium acetate excess in

2-methoxyethanol as the common solvent. The 200–250 nm thick films crystallized in perovskite phase upon heating at 750 °C for 5 min in a rapid thermal annealing furnace notwithstanding the amount of the excess or the choice of the alkali reagent. However, the amount of the alkali excess strongly influenced the microstructure and orientation of the perovskite phase, consequently it was also reflected in functional properties of the films and in their phase-transitional behaviour.[12,13] The films, prepared from the solutions with 0 or 5 mole % alkali excess, consisted of equiaxed grains of about 50 nm across, while the films, prepared from the solutions with 10 mole % alkali excess had columnar microstructures, with the lateral grain size almost equal to the film thickness, see Figure 1. The degree of {100} orientation was much more pronounced in the latter films.[12]

A study of KNN thin-film precursors has been undertaken in order to elucidate the origin of the observed differences in the films, presumably stemming from different chemical composition of the coating solutions. Chemical composition of the liquid and as-dried precursors was probed by Fourier-transform infrared spectroscopy. Furthermore, thermo gravimetric and differential thermal analyses in combination with evolved gas analysis by mass spectrometry of the as-dried precursors containing different amounts of alkali excess were performed and compared.

2. Experimental

Potassium acetate (CH_3COOK, 99+%, Sigma Aldrich), sodium acetate (CH_3COONa, 99.5%, Fluka) and Nb-pentaethoxide ($Nb(OCH_2CH_3)_5$, 99.99%, Starck) were weighted in a stoichiometric ratio and dissolved in 2-methoxyethanol. All manipulations and reactions were performed in a dry inert atmosphere. After 4 hours of refluxing and distillation of by-products, the concentration of the solution was adjusted to 0.4 M. After cooling to room temperature, the alkali acetates in excess were added. Thus the colourless stable solutions without any alkali excess and with 5 mole % excess of K, 5 mole % Na, 10 mole % K, and 10 mole % Na were prepared, further denoted as Stoich-, 5K-, 5Na-, 10K-, and 10Na-KNN, respectively. The details of the synthesis are described in our previous paper,[12]

For Fourier-transform infrared spectroscopy (FT-IR) and thermal analysis (TA), the solutions were dried at 60 °C for 30 min, at 90 °C for 60 min and at 110 °C for 60 min. The alkali acetates were dried at 200 °C to constant mass.

The FTIR spectra were recorded on two Nicolet 6700 spectrometers. The liquid samples were recorded in the attenuated total-reflection (ATR) mode with the diamond crystal in the ranges 600–1800 cm^{-1} and 2300–4000 cm^{-1}. In the interval 1800–2300 cm^{-1} the bands of the diamond crystal are present and this interval was cut from the spectra. Note that the liquid samples do not have any important bands in this range. The spectra of the as-dried samples were recorded with another device in transmittance mode. The spectra were taken from thin transparent KBr pellets containing approximately 0.5 wt. % samples in the 400–4000 cm^{-1} range.

The samples were analysed by simultaneous thermogravimetry (TG), derivative thermogravimetry (DTG)
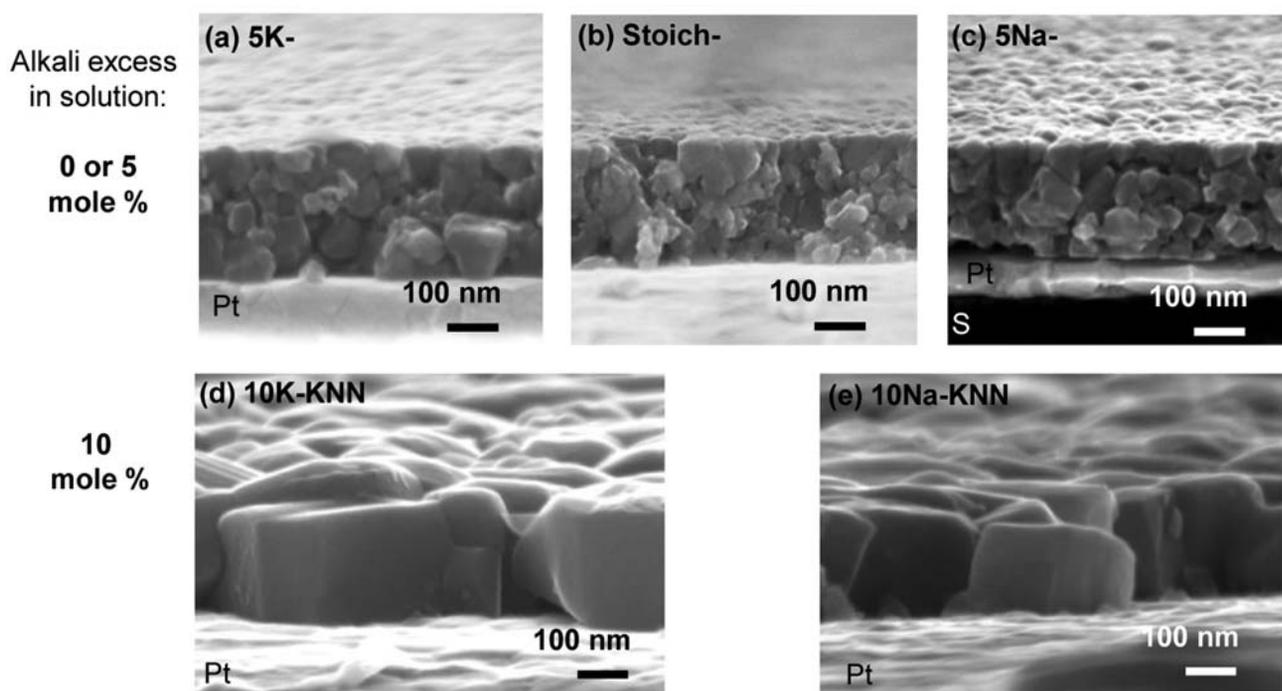

Figure 1: Cross-section microstructures of (a) 5K-, (b) Stoich-, (c) 5Na-, (d) 10K and (e) 10Na-KNN thin films. Based on reference[12].

and differential thermal analysis (DTA), (Netzsch STA 409), coupled with a quadropole mass spectrometer (BalzersThermostar GSD 300 T) through a heated quartz capillary, for the analysis of the evolved gases, EGA. The samples of about 50 mg were heated in PtRh crucibles at the heating rate of 10 °C/min to 750 °C in a flowing air atmosphere.

3. Results and Discussion

The Stoich-KNN solution precursor was synthesized upon the reaction of alkali acetates and Nb-ethoxide in the ether-alcohol solvent. In addition to the ester-elimination reaction between the acetate and alkoxide groups,[14] also partial transalcoholysis, i.e., exchange of ethoxide groups with methoxyethoxide could be expected.[15] Upon drying in air the solvent evaporated, and reactions with humidity could be expected, resulting in the formation of oxo- and/or hydroxo- species.[16] Assuming a stoichiometric reaction between the alkali and niobium reagents the dried precursor could be roughly described as $K_{0.5}Na_{0.5}Nb(OCH_2CH_3)_x(OCH_2CH_2OCH_3)_y(O)_z(OH)_w$, where $x + y + z + w = 6$. Note that possible oligomerisation and/or solvation have not been taken into account.

Infrared spectroscopy was used to obtain insight in chemical composition of the KNN sols and as-dried precursors. The latter were amorphous, as confirmed by X-ray diffraction (patterns not shown here). In Figure 2 the FT-IR spectra of the sols and the solvent are presented. The FT-IR spectrum of the solvent 2-methoxyethanol (CH_3-O-CH_2-CH_2-OH) shows a broad band with the maximum at 3406 cm^{-1} assigned to vibrations of O-H bonds in alcohols. The broad band in the range 2700–3000 cm^{-1} can be decomposed in the following bands: at 2960 and 2872 cm^{-1}, assigned to the asymmetric and symmetric stretching of CH_3– groups; at 2925 cm^{-1} a band associated with asymmetric stretching in –CH_2– groups and at 2826 cm^{-1} a band assigned to symmetric stretching of the CH_3– group in ethers (CH_3-O-CH_2). The bands at 1455 cm^{-1} can be attributed to scissoring motions of –CH_2– groups. The bands in the 1232 –1420 cm^{-1} range are assigned to scissoring and twisting motions of C-H bonds in the CH_2-OH group. The vibrations corresponding to C-O-C bonds in the ether group lead to a group of bands in the range 1060–1193 cm^{-1}. The band at 1018 cm^{-1} is assigned to stretching of (C-OH) bonds while the bands at 963, 926, 890 and 831 cm^{-1} are assigned to stretching of (C-O) bonds. The assignations of bands are in agreement with the bands evidenced in organic compounds as alcohols and ethers.[17,18]

FTIR spectra of all KNN sols look similar. In addition in the spectrum of KNN sols two new bands at 1741 and 1578 cm^{-1} appear that can be assigned to asymmetric and symmetric stretching of C=O bond in the acetate group, introduced by the alkali reagents. The band assig-

ned to stretching of the (C-O) bond that appears in spectrum of the solvent at 926 cm^{-1} was shifted in case of the KNN sol to 916 cm^{-1}; probably due to interaction in solution of the acetates with the solvent.
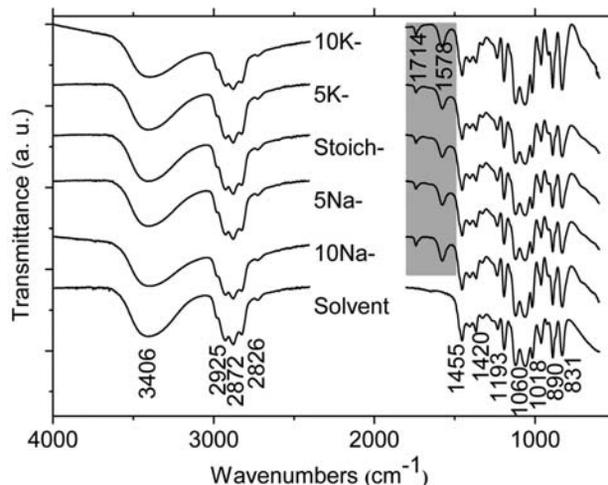

Figure 2: FT-IR spectra of the KNN sols and the solvent recorded in the ATR mode with the diamond crystal.

In Figure 3 the FT-IR spectra of the dried precursors are collected. One may note that the characteristic bands assigned to the organic components of the studied solutions vanished, except those assigned to the COO- vibrations (1560 cm^{-1} and 1411 cm^{-1}) stemming from alkali acetates. The presence of adsorbed water and hydroxyl groups are also noticed, as well as the absorption bands around 800, 643 and 522 cm^{-1}, characteristic for Nb–O stretching modes. The results are in agreement with infrared and Raman data reported for KNN nanoparticles,[19,20] niobate glass-ceramics[21,22] and niobium silicate glasses.[23–28]
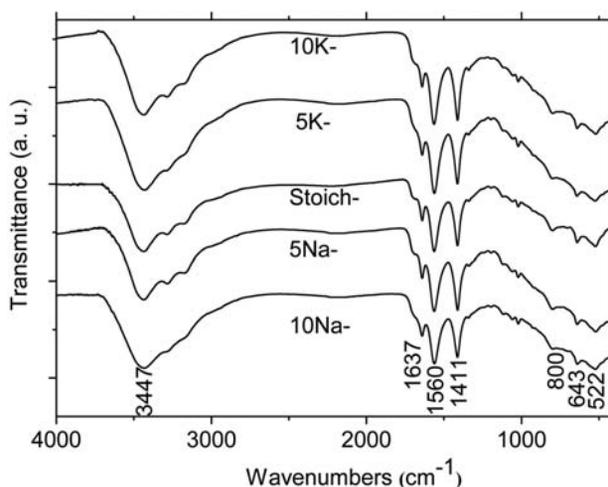

Figure 3: FT-IR spectra of the as-dried KNN precursors, recorded on KBr pellets, in transmission mode.

In the FTIR spectra of the KNN sols, the two bands at 1741 and 1578 cm^{-1} are assigned to the ν_{as}(COO$^-$) and ν_{sym}(COO$^-$) groups.[29,30] In the as-dried samples these bands are shifted to 1560 and 1411 cm^{-1} showing the interaction of the reagents by formation of complexes. According to the data of raw materials, the bands at 1432, 1460 and 1570 cm^{-1} in sodium acetate and at 1425 and 1590 cm^{-1} in potassium acetate were assigned to (COO$^-$) groups. The positions of bands in liquid and in as-dried samples were displaced as compared to the positions of bands in raw materials, confirming therefore formation of acetate-based heteropolynuclear complexes.

The FTIR spectra of both liquid and dried KNN precursors were quite similar and did not reveal specific features which could be attributed to alkali-acetate excess. Further analysis of the dried precursors was performed by TG/DTA/EGA.

The thermal analysis curves of the dried Stoich-KNN precursor are collected in Figure 4. The sample lost 20.45% of mass upon heating to 750 °C. Its thermal decomposition occurred stepwise: the mass loss from room temperature to 200 °C was 2.20%, from 200 °C to 470 °C 14.90%, and upon further heating to the final temperature 3.35%.

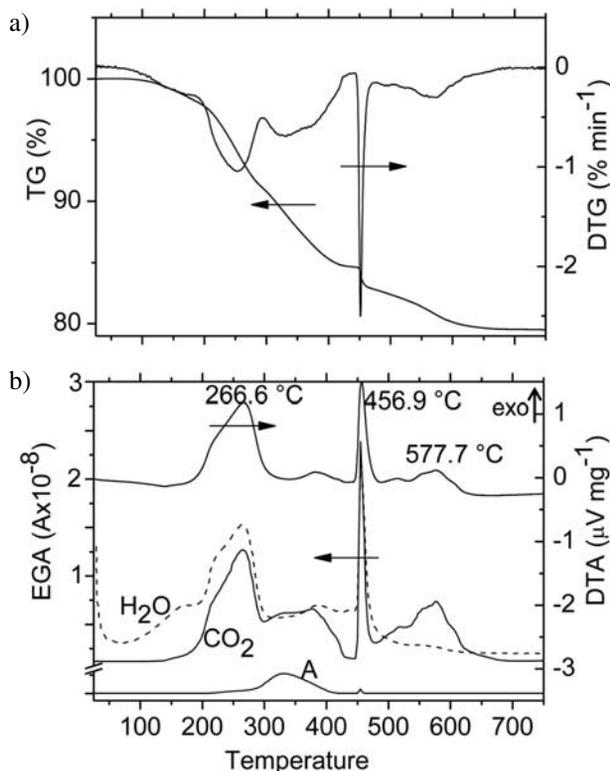The thermal effects recorded by DTA included a weak endothermic peak between room temperature and 200 °C, and a succession of exothermic peaks between 200 °C and 630 °C. We observed a strong, broad peak at 266.6 °C, a strong, sharp peak at 456.9 °C and another strong peak at 577.7 °C.

We followed the mass peaks of water (m/e$^+$ 18), carbon dioxide (m/e$^+$ 44) and acetone (m/e$^+$ 58). Between room temperature and 200 °C, in the first step of mass loss, predominantly water was evolved. In the next step, from 200 °C to 480 °C, which corresponds to about 74% of the total mass loss, water and carbon dioxide were evolved in a series of steps. Traces of acetone were also detected in this temperature range. Upon further heating to 630 °C only carbon dioxide peak was detected.

Thermal analysis of the as-dried Stoich-KNN precursor revealed that upon heating to 200 °C evaporation of water and residual solvent occurred as confirmed by a broad endothermic peak. Upon further heating from ~200 °C to ~480 °C, the evolution of water, carbon dioxide and traces of acetone confirmed thermal oxidation of organic species, i.e. alkoxide and acetate groups, associated with broad exothermic DTA peaks. Note that acetone is an intermediate product of the acetate group decomposition and it has been detected in earlier studies of thermal decomposition of other heterometallic alkoxide-acetate derived precursors.[31–33] An abrupt mass loss of 2%, accompanied by a strong sharp exothermic DTA peak and simultaneous evolution of water and carbon dioxide in the temperature interval between ~450 and ~480 °C is attributed to oxidation of residual organic species, however based on thermal analysis only we could not conclude which reactions took place, or if also crystallization simultaneously occurred. From about 470 °C to 630 °C thermal oxidation of carbonaceous residues occurred as evidenced by predominant evolution of carbon dioxide and a broad DTA exotherm. Chowdhury performed a systematic TA study of KNN precursors, prepared from metal ethoxides in 2-methoxyethanol with different refluxing times, from 0 h to 70 h. It is worthwhile to note that he also detected a strong exothermic double peak and a mass loss of a few % at about 500 °C however, only CO$_2$ was evolved in his case. He attributed it to coupled carbonate decomposition and crystallization events.[34]

Before analysing the alkali-excess KNN precursors, thermal decompositions of potassium and sodium acetates were recorded by TG/DTA. Note that the final temperature of 600 °C was selected for analyses to avoid possible contamination of the instrument by alkali vapours. According to literature sodium acetate decomposes to oxide with the carbonate as the intermediate phase.[35]

The TG/DTA curves of both alkali acetates are quite similar, as evident from Figure 5. The DTA curves of potassium and sodium acetate exhibit an endothermic peak at 306.1 and 330.8 °C due to melting.[35]

We observe that the major mass losses of both samples occur between approximately 420 °C and 540 °C, accompanied by strong exothermic peaks. The total mass losses of 32.5% and 36.4% for potassium and sodium ace-
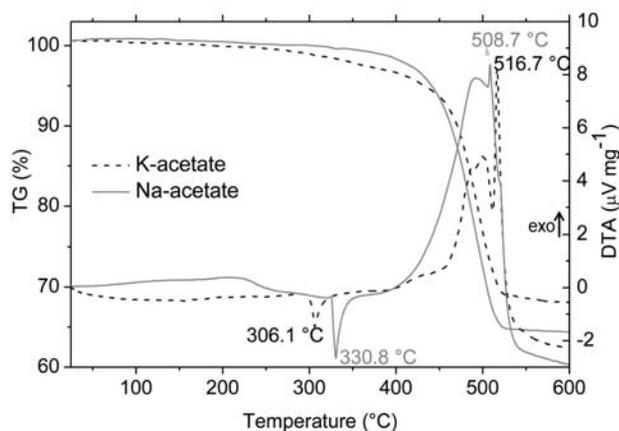

Figure 4: (a) TG, DTG and (b) DTA and EGA curves of the Stoich-KNN precursor. A denotes evolution of acetone.

Figure 5: TG/DTA curves of potassium and sodium acetates.

tate, respectively, are larger than the theoretical values corresponding to the decomposition of respective acetates to carbonates (29.6% and 35.4%). This slight increase is attributed to adsorbed humidity. Evaporation of water upon heating to about 200 °C is especially pronounced in the case of potassium acetate.

Thermal decompositions of the potassium-excess KNN precursors are collected in Figure 6, a. Note that the TA curves of the Stoich-KNN are included for easier comparison. The total mass losses upon heating from room temperature to 750 °C were 22.46% and 22.58% for the 5K- and 10K-KNN, respectively. There are some differences in the TG/DTA curves mainly between 180 °C and 330 °C. The rate of mass loss increases with increasing amount of potassium-excess. We observe a sequence of a weaker and a stronger exothermic DTA peak at 207.5 and 275.5 °C in the case of 5K-KNN sample and a similar one, but more exothermic and shifted to slightly lower

temperatures for the 10-KNN sample, i.e. 199.6 and 247.4 °C, respectively. Both potassium-excess samples exhibit a strong, sharp exothermic peak at ~450 °C related to a small mass loss, similar as the Stoich-KNN. Upon heating above 480 °C, the TG and DTA curves had quite similar sequences of peaks in all three samples. The EGA analysis revealed that evolution of carbon dioxide was detected up to 700 °C for the 10K-KNN and only up to 630 °C for the 5K-KNN (not shown here) and Stoich-KNN. We could conclude that the addition of potassium acetate to the Stoich-KNN solution resulted in changes in the TG/DTA curves especially between ~200 and ~330 °C, indicating that some interaction between the heterometallic complex and potassium acetate occurred. Note that the acetate itself was stable upon heating to about 400 °C, see Figure 5.

The TA curves of the 5Na- and 10Na-precursors are collected in Figure 6, b. The data for Stoich-KNN are included for comparison. The total mass losses upon heating from room temperature to 750 °C were 20.51% and 22.50% for the 5Na- and 10Na-KNN, respectively. The main difference between the two alkali-excess samples and the Stoich-KNN is in the ~180 °C and ~400 °C interval. Contrary to the potassium-excess samples, the major mass loss of the 5Na-KNN sample is slightly up-shifted in relation to Stoich-KNN, with the DTA exo-peaks at 280.3 and 351.6 °C. The intensive mass-loss of the 10Na-KNN starts at a lower temperature than for the Stoich-KNN, and the major exo-peak is at 248.5 °C, almost 20 °C lower than that of Stoich-KNN. At higher temperatures the sequences of mass losses and DTA peaks of sodium-excess samples are quite similar to those of Stoich-KNN. Similar as in the case of potassium-excess samples we can conclude that the sodium-excess samples exhibit different thermal decomposition pathways than the Stoich-KNN. Furthermore, alt-
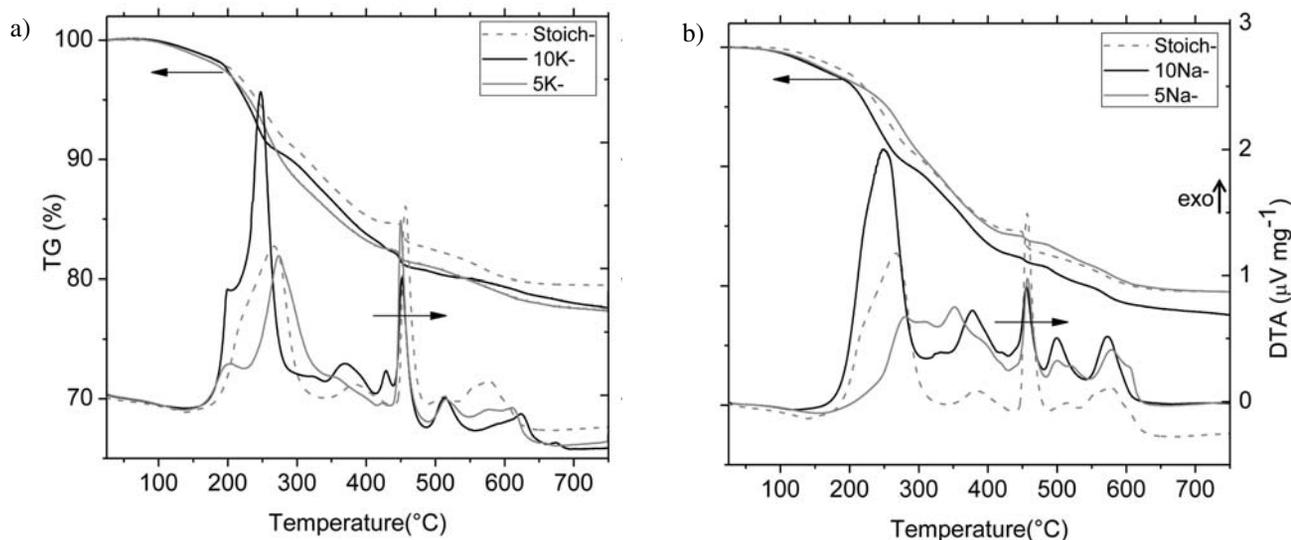

Figure 6: TG/ DTA curves of (a) 5K- and 10K-KNN and (b) 5Na- and 10Na-KNN precursors. The corresponding curves of the Stoich-KNN are added for comparison.

hough there are some differences between the 5K- and 5Na samples, we observe a similar influence of the amount of alkali-excess on the thermal decompositions. This observation is in agreement with the noted differences in the microstructures of the 5K- or 5Na- thin films as compared to the 10K- and 10Na-KNN films,[12] see Figure 1.

5. Summary

Infrared spectroscopy and thermal analysis were used to study the KNN thin-film precursors, synthesized from stoichiometric mixtures of sodium and potassium acetates, and niobium ethoxide in 2-methoxyethanol with 0, 5 or 10 mole % of sodium or potassium acetate excess in order to elucidate the origin of the observed differences in microstructures of the obtained films.

As expected, the FTIR spectra of KNN sols revealed the presence of acetate groups, which were introduced by the alkali reagents and a slight shift in the band assigned to stretching of the (C-O) bond, probably due to interaction of the acetates with the solvent. The FT-IR results of the dried KNN powders support the formation of acetate-based heteropolynuclear complexes.

The thermal decomposition of all KNN precursors occurred stepwise: in the first step, up to 200 °C, water and residual solvent evaporated and upon further heating from ~200 °C to ~480 °C, thermal oxidation of organic species, i.e. alkoxide and acetate groups took place. The TG/DTA curves of potassium and sodium acetates were also recorded and revealed melting at 306.1 and 330.8 °C, respectively, and the decomposition between 420 °C and 540 °C in both cases.

Addition of acetate excess to the stoichiometric KNN precursor resulted in changes in the TG/DTA curves especially between ~200 and ~330 °C, indicating some interaction between the heterometallic complex and acetate. As compared to the stoichiometric and 5 mole % alkali excess precursors, the intensive mass-loss of the 10K- and 10Na-KNN started at a lower temperature and the main DTA peaks at around 248 °C are more exothermic and down-shifted.

Although there are some differences between the 5K- and 5Na- samples, we observed a similar influence of the amount of alkali-excess on the thermal decompositions. This observation is in agreement with the noted differences in the microstructures of the films from solutions with different amounts of alkali excesses.

6. Acknowledgements

7. References

1. J. Roedel, W. Jo, K. T. P. Seifert, E. M. Anton, T. Granzow and D. Damjanovič, *J Am Ceram Soc*, **2009**, *92*, 1153–1177.
2. J. F. Scott, *Science*, **2007**, *315*, 954–959.
3. P. Muralt, *J. Micromech. Microeng.*, **2000**, *10*, 136–146.
4. L. Egerton and D. M. Dillon, *J Am Ceram Soc*, **1959**, *42*, 438.
5. S. Zhang, R. Xia and T. R. Shrout, *J Electroceram*, **2007**, *19*, 251–257.
6. C. R. Cho and A. Grishin, *J Appl Phys*, **2000**, *87*, 4439–4448.
7. K. Shibata, K. Suenaga, A. Nomoto and T. Mishima, *Jpn J Appl Phys*, **2009**, *48*, 121408.
8. Y. Nakashima, W. Sakamoto, T. Shimura and T. Yogo, *Jpn J Appl Phys*, **2007**, *46*, 6971.
9. C. W. Ahn, S. Y. Lee, H. J. Lee, A. Ullah, J. S. Bae, E. D. Jeong, J. S. Choi, B. H. Park and I. W. Kim, *J Phys D Appl Phys*, **2009**, *42*, 215304.
10. L. čakare-Samardžija, B. Malič and M. Kosec, in *Ferroelectrics*, Bled, 2008, pp. 113–118.
11. L. Wang, K. Yao, P. C. Goh and W. Ren, *J Mater Res*, **2009**, *24*, 3516–3522.
12. A. Kupec, B. Malič, J. Tellier, E. Tchernychova, S. Glinšek and M. Kosec, *J. Am. Ceram. Soc.*, **2012**, *95*, 515.
13. A. Kupec, P. Gemeiner, B. Dkhil and B. Malič, *Thin Solid Films*, **2013**, *539*, 317–322.
14. B. Malič and S. Glinšek, in T. Schneller, R. Waser, M. Kosec and D. Payne (Ed.): Chemical Solution Deposition of Functional Oxide Thin Films, Springer Vienna, **2013**, pp. 51–69.
15. M. Sedlar and M. Sayer, *J. Sol-gel Sci. Techn.*, **1995**, *5*, 27–40.
16. C. J. Brinker and G. W. Scherer, Sol-gel science: The physics and chemistry of sol-gel processing, Academic Press, San Diego, **1990**.
17. M. Zaharescu and O. C. Mocioiu, in T. Schneller, R. Waser, M. Kosec and D. Payne (Ed.): Chemical Solution Deposition of Functional Oxide Thin Films, Springer Vienna, **2013**, pp. 213–231.
18. J. Coates, in R. A. Meyers (Ed.): Encyclopedia of Analytical Chemistry: Applications, Theory and Instrumentation, Wiley& Sons Ltd, Chichester, **2000**, pp. 10822–10828.
19. F. Rubio-Marcos, J. J. Romero, M. S. Martín-Gonzalez and J. F. Fernández, *J. Eur. Ceram. Soc.*, **2010**, *30*, 2763–2771.
20. A. Chowdhury, J. Bould, M. G. S. Londesborough, E. Večerníková and S. J. Milne, *Mater. Chem. Phys.*, **2010**, *124*, 159–162.
21. J. F. Liu, X. L. Li and Y. D. Li, *J. Cryst. Growth*, **2003**, *247*, 419–424.
22. M. Tatsumisago, A. Hamada, T. Minami and M. Tanaka, *J. Non-Cryst. Solids*, **1983**, *56*, 423–428.
23. L. F. Santos, L. Wondraczek, J. Deubener and R. M. Almeida, *J. Non-Cryst. Solids*, **2007**, *353*, 1875–1881.
24. M. P. F. Graça, M. G. Ferreira da Silva, A. S. B. Sombra and M. A. Valente, *J. Non-Cryst. Solids*, **2007**, *353*, 4390–4394.
25. M. P. F. Graça, M. G. F. d. Silva and M. A. Valente, *J. Non-Cryst. Solids*, **2008**, *354*, 901–908.
26. M. P. F. Graça, M. Peres, M. A. Valente, A. J. Neves and T. Monteiro, *J. Non-Cryst. Solids*, **2008**, *354*, 5244–5246.

27. R. C. C. Figueira, M. P. F. Graça, L. C. Costa and M. A. Valente, *J. Non-Cryst. Solids*, **2008**, *354*, 5162–5164.

28. A. Aronne, V. N. Sigaev, B. Champagnon, E. Fanelli, V. Califano, L. Z. Usmanova and P. Pernice, *J. Non-Cryst. Solids*, **2005**, *351*, 3610–3618.

29. K. Nakamoto, Infrared and Raman Spectra of Inorganic and Coordination Compounds, Part B, Applications in Coordination, Organometallic and Bioinorganic Chemistry, John Wiley & Sons Inc, , Hoboken, **2009**.

30. G. B. Deacon and R. J. Philips, *Coord. Chem. Rev.*, **1980**, *33*, 227–250.

31. P. R. Coffman, C. K. Barlingay, A. Gupta and S. K. Dey, *J. Sol-gel Sci. Techn.*, **1996**, *6*, 83–106.

32. B. Malič, M. L. Calzada, J. Cilenšek, L. Pardo and M. Kosec, *Adv. Appl. Ceram.*, **2010**, *109*, 147–151.

33. B. Malič, M. Mandeljc, G. Dražič, M. Škarabot, I. Muševic and M. Kosec, *Integr. Ferroelectr.*, **2008**, *100*, 285–296.

34. A. Chowdhury, J. Bould, M. G. S. Londesborough and S. J. Milne, *Chem. Mater.*, **2010**, *22*, 3862–3874.

35. M. D. Judd, B. A. Plunkett and M. I. Pope, *J. Therm. Anal.*, **1974**, *6*, 555–563.

Povzetek

Tekoče prekurzorje $(K_{0.5}Na_{0.5})NbO_3$ smo pripravili iz alkalijskih acetatov in niobijevega alkoksida v stehiometričnem razmerju, Na/K/Nb je 0,5/0,5/1, in s prebitkom 5 ali 10 molskih % kalijevega ali natrijevega acetata. Infrardeča spektroskopija s Fourierjevo transformacijo (FTIR) sušenih prekurzorjev je potrdila prisotnost acetatnih in hidroksilnih skupin. Termični razpadi sušenih raztopin v zraku potekajo v stopnjah. Manjšo izgubo mase, zaznano v območju med sobno temperaturo in okoli ~200 °C, pripisujemo izhlapevanju topila. Največje izgube mas v območju med 200 °C in 400 °C so posledica termične oksidacije organskih skupin. V tem območju smo najmočnejše eksotermne odklone zaznali pri ~250 °C in ~450 °C, kar je skoraj 200 °C nižje od začetka termičnega razpada alkalijskih acetatov. Slednje potrjuje tvorbo heterometalnih kompleksov, v skladu s FTIR analizo. Raziskava je pokazala, da količina in v manjši meri tudi tip prebitka vplivata na termični razpad organskih skupin, predvsem v območju med ~200 °C in ~400 °C.